

## LOCAL BUCKLING ANALYSIS OF THICK ANISOTROPIC PLATES USING COMPLEX FINITE STRIP METHOD\*

M. AZHARI\*\* AND KH. KASSAEI

Dept. of Civil Engineering, Isfahan University of Technology, Isfahan, I. R. of Iran  
Email: mojtaba@cc.iut.ac.ir

**Abstract** – An analysis of buckling for thick anisotropic plates subjected to arbitrary loading is presented. The analysis employs the complex finite strip method which utilizes complex harmonic functions in the longitudinal direction, a cubic polynomial in the transverse direction and a parabolic distribution of the transverse shear strains through the thickness of the thick plate based on the higher-order shear deformation theory. The method is programmed to investigate local buckling of square and long thick plates subjected to compression bending and shear stresses. Examples of the accuracy of the method with an increasing number of strips are presented. The method is then applied to study the local instability of thick orthotropic plates under compression and shear with different boundary conditions. Local instability interaction between compression and shear, and bending and shear in thick orthotropic plates is investigated.

**Keywords** – Local instability, thick plate, shear deformation theory, complex finite strip method,

### 1. INTRODUCTION

With the modern trend of employing layered composites in the aerospace and automotive industries, the prediction of local buckling of such structures is attracting great attention from many researchers. Several theoretical investigations have been presented on the buckling of anisotropic plates under combined loading. Zurieck [1] reported a complete review of the application of the layered composites.

The earliest general method for the local buckling of composite plates under arbitrary loading was the finite element method [2]. While the finite element method provides a general framework, it invariably results in problems which possess a large number of degrees of freedom, from which extraction of the buckling stress may be expensive. Vibration analysis of a thick plate with an interior cut-out using a quadratic element of eight nodes was investigated by Chang and Chang [3]. Local buckling of anisotropic plates has been studied by Noor [4], Stein [5] and Nemeth [6].

In the analysis of thick plates, the neglect of transverse shear strains could lead to an overestimation of the natural frequencies and critical buckling loads because of the low transverse shear moduli [7]. This difficulty was overcome by using a first order shear deformation theory in which constant shear strains through the plate thickness are considered by Reddy and Chandrashekhara [8] and [9]. Since the first order shear deformation theory does not account for the parabolic variation of transverse shear strain through the thickness, the second shear deformation theory was proposed by Sing *et al.* [10].

Although local buckling analyses can be performed for nearly any thick plate configuration using a general finite element method, the finite strip method is more attractive and economically feasible for prismatic plate assemblies because of the significant reduction in the buckling degrees of freedom [11]. Zeggane and Sridharan [12] presented an efficient formulation to predict the buckling behavior of long shear deformable laminated anisotropic plates. In their analysis, the effect of shear locking was eliminated by the use of higher Lagrangian polynomials. Akhras *et al.* [13] presented a finite strip method for the vibration and stability analyses of anisotropic laminated composite plates according to the higher order shear deformation

---

\*Received by the editors November 13, 2002 and in final revised form August 24, 2003

\*\*Corresponding author

theory.

The spline finite strip method, in which the longitudinal trigonometric series is replaced by a linear combination of  $B_3$ -spline functions and transverse polynomials, was employed to study buckling and vibration of rectangular composite laminated plates under combined loading by Daw and Wang [14] and [15] Wang and Daw [16]. Azhari *et al.* [17] studied local buckling of composite laminated plate assemblies using the spline finite strip method. Since in their analysis transverse shear strains were neglected, the critical buckling loads were overestimated. More recently, Saadatpour *et al.* [18] presented a numerical method for the analysis of general quadrilateral, moderately thick orthotropic plates having arbitrary boundary conditions. Their procedure is based on the application of the Rayleigh-Ritz method in conjunction with the Reissner-Mindlin thick plate theory.

In the present paper, the complex finite strip method developed by Plank and Wittrick [19] is extended for the analysis of very thick plates. The higher order shear deformation theory that accounts for a parabolic variation of the transverse shear strains throughout the thickness and zero transverse shear stresses on the surface of the plate is employed. The advantage of this approach over the formulations of Akhras *et al.* [13] is the ease with which it can handle shear. The application of the method is shown by examining a long, thick rectangular plate under compression and shear.

## 2. THEORY

### a) General

The complex finite strip method for buckling analysis of thin-walled structures was originally developed by Plank and Wittrick [19]. Azhari and Bradford [20] fully formulated the stiffness and stability matrices for a strip using bubble functions for the case of elastic buckling analysis and thin plates. In this section, the relevant changes to include the higher order shear deformation theory for thick-plate analysis are presented. Figure 1 shows the geometry and prebuckling stresses, while Fig. 2 shows the system of displacement of a typical complex finite strip which forms part of a thick plate assembly.

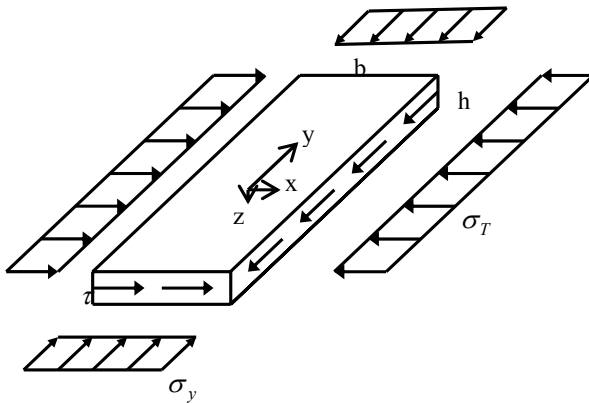


Fig.1 Prebuckling stresses on a strip

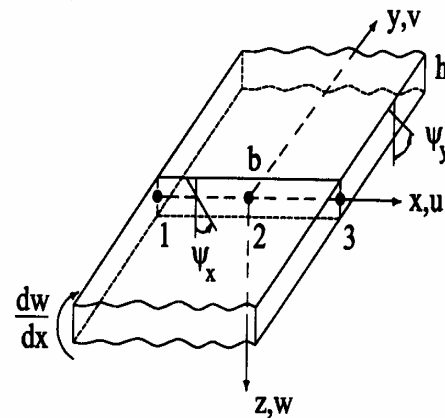


Fig.2 Prebuckling system of displacements on a strip

### b) Kinematics

The strip is subjected, on its edges, to a system of perturbation forces and displacements. The vectors of perturbation forces  $\mathbf{p}$  and corresponding displacements  $\mathbf{d}$  of the edges are defined as

$$\mathbf{p} = \{p_{x1}, ip_{y1}, p_{z1}, m_1, T_{x1}, iT_{y1}, p_{x2}, ip_{y2}, T_{x2}, iT_{y2}, p_{x3}, ip_{y3}, p_{z3}, m_3, T_{x3}, iT_{y3}\} \quad (1)$$

$$\mathbf{d} = \left\{ u_1, iv_1, w_1, \left(\frac{\partial w}{\partial x}\right)_1, \psi_{x1}, i\psi_{y1}, u_2, iv_2, \psi_{x2}, i\psi_{y2}, u_3, iv_3, w_3, \left(\frac{\partial w}{\partial x}\right)_3, \psi_{x3}, i\psi_{y3} \right\} \quad (2)$$

where the second subscripts denote the edge numbers,  $p_x$ ,  $p_y$  and  $p_z$  are the forces in the  $x$ ,  $y$  and  $z$  directions, respectively;  $m$  is the moment about  $y$ .  $u$ ,  $v$  and  $w$  are the displacements in the  $x$ ,  $y$  and  $z$  directions, respectively;  $\psi_x$  and  $\psi_y$  are the rotations of the normal to the mid-plane about the  $y$  and  $x$  axes, respectively. The introduction of ( $i = \sqrt{-1}$ ) in the vectors  $\mathbf{p}$  and  $\mathbf{d}$  automatically incorporates a 90 degree phase difference between the  $u$  and  $v$  displacements.

The displacement field, which includes classical plate theory and accounts for the parabolic variation of transverse shear strain through the thickness of the plate, is assumed to be

$$u_o = \text{Re}\{\mathbf{XJd}e^{i\eta}\}, \quad v_o = \text{Re}\{\mathbf{YJd}e^{i\eta}\} \quad \text{and} \quad w = \text{Re}\{\mathbf{ZJd}e^{i\eta}\} \quad (3)$$

$$\psi_x = \text{Re}\{\mathbf{R}_x \mathbf{Jd}e^{i\eta}\} \quad \text{and} \quad \psi_y = \text{Re}\{\mathbf{R}_y \mathbf{Jd}e^{i\eta}\} \quad (4)$$

where  $\text{Re}\{\}$  denotes the real part of the quantity inside the brackets;  $\mathbf{X}$ ,  $\mathbf{Y}$ ,  $\mathbf{Z}$ ,  $\mathbf{R}_x$  and  $\mathbf{R}_y$  are the interpolation matrices defined by Eqs. (5);  $\mathbf{J}$  is a  $16 \times 16$  matrix defined by Eq. (6) and  $\eta = \pi y / \lambda$  in which  $\lambda$  is the buckling half-wavelength. It should be noted that when the boundary conditions along loaded edges are not simply supported, the series functions to satisfy the boundary conditions are used instead of  $e^{i\eta}$  [21].

$$\mathbf{X} = \begin{bmatrix} \frac{1}{2}\xi(\xi-1) & 0 & 0 & 0 & 0 & 0 & 1-\xi^2 & 0 & 0 & 0 & \frac{1}{2}\xi(\xi+1) & 0 & 0 & 0 & 0 & 0 \end{bmatrix} \quad (5a)$$

$$\mathbf{Y} = \begin{bmatrix} 0 & \frac{1}{2}\xi(\xi-1) & 0 & 0 & 0 & 0 & 1-\xi^2 & 0 & 0 & 0 & \frac{1}{2}\xi(\xi+1) & 0 & 0 & 0 & 0 \end{bmatrix} \quad (5b)$$

$$\mathbf{Z} = \begin{bmatrix} 0 & 0 & \frac{1}{4}(1-\xi)^2(2+\xi) & \frac{b}{8}(1-\xi)^2(1+\xi) & 0 & 0 & 0 & 0 & 0 & 0 & 0 & 0 & 0 & 0 & 0 & 0 \\ \frac{1}{4}(1-\xi)^2(2+\xi) & -\frac{b}{8}(1-\xi)(1+\xi)^2 & 0 & 0 & 0 & 0 & 0 & 0 & 0 & 0 & 0 & 0 & 0 & 0 & 0 & 0 \end{bmatrix} \quad (5c)$$

$$\mathbf{R}_x = \begin{bmatrix} 0 & 0 & 0 & 0 & \frac{1}{2}\xi(\xi-1) & 0 & 0 & 0 & 1-\xi^2 & 0 & 0 & 0 & 0 & 0 & \frac{1}{2}\xi(\xi+1) & 0 \end{bmatrix} \quad (5d)$$

$$\mathbf{R}_y = \begin{bmatrix} 0 & 0 & 0 & 0 & 0 & \frac{1}{2}\xi(\xi-1) & 0 & 0 & 0 & 1-\xi^2 & 0 & 0 & 0 & 0 & 0 & \frac{1}{2}\xi(\xi+1) \end{bmatrix} \quad (5e)$$

in which  $\xi = 2x/b$ .

$$\mathbf{J} = [1 \quad -i \quad 1 \quad 1 \quad 1 \quad -i \quad 1 \quad -i \quad 1 \quad -i \quad 1 \quad -i \quad 1 \quad 1 \quad 1 \quad -i] \quad (6)$$

According to the higher-order shear deformation theory, the displacements at any point ( $\xi, \eta, z$ ) of a laminate are given by Reddy *at al.* [9]

$$u = u_o + z\psi_x - \frac{4z^3}{3h^2} \left( \psi_x + \frac{\partial w}{\partial x} \right) \quad \text{and} \quad v = v_o + z\psi_y - \frac{4z^3}{3h^2} \left( \psi_y + \frac{\partial w}{\partial y} \right) \quad (7)$$

It should be noted that the Hermitian cubic polynomials used as the interpolation function of  $w$  in the  $x$  direction, guarantee inter-element continuity for the transverse displacement  $w$  and for its first derivatives  $\partial w / \partial x$  and  $\partial w / \partial y$ . The linear and nonlinear buckling strain vectors  $\boldsymbol{\varepsilon}_L$  and  $\boldsymbol{\varepsilon}_{NL}$  are given by

$$\boldsymbol{\varepsilon}_L = \left\langle \frac{\partial u}{\partial x}; \frac{\partial v}{\partial y}; \frac{\partial u}{\partial y} + \frac{\partial v}{\partial x}; \frac{\partial w}{\partial y} + \frac{\partial v}{\partial z}; \frac{\partial w}{\partial x} + \frac{\partial u}{\partial z} \right\rangle^T \quad (8a)$$

$$\boldsymbol{\varepsilon}_{NL} = \left\langle \frac{1}{2} \left[ \left( \frac{\partial u}{\partial x} \right)^2 + \left( \frac{\partial v}{\partial x} \right)^2 + \left( \frac{\partial w}{\partial x} \right)^2 \right]; \frac{1}{2} \left[ \left( \frac{\partial u}{\partial y} \right)^2 + \left( \frac{\partial v}{\partial y} \right)^2 + \left( \frac{\partial w}{\partial y} \right)^2 \right]; \frac{1}{2} \left( \frac{\partial u}{\partial x} \frac{\partial u}{\partial y} + \frac{\partial v}{\partial x} \frac{\partial v}{\partial y} + \frac{\partial w}{\partial x} \frac{\partial w}{\partial y} \right) \right\rangle^T \quad (8b)$$

Using Eqs. (3), (4) and (7), the linear strain vector  $\boldsymbol{\varepsilon}_L$  becomes

$$\boldsymbol{\varepsilon}_L = \text{Re}(\boldsymbol{\Gamma} \mathbf{J} d e^{i\eta}) \quad (9)$$

where  $\boldsymbol{\Gamma}$  is a  $5 \times 6$  matrix defined by

$$\boldsymbol{\Gamma} = \begin{bmatrix} \frac{2}{b} \left[ \mathbf{X}' + \left( z - \frac{4z^3}{3h^2} \right) \mathbf{R}'_x - \frac{8z^3}{3h^2 b} \mathbf{Z}'' \right] \\ \frac{\pi}{\lambda} \left[ \left( \mathbf{Y} + \left( z - \frac{4z^3}{3h^2} \right) \mathbf{R}'_y \right) i + \frac{4\pi z^3}{3h^2 \lambda} \mathbf{Z} \right] \\ \frac{2}{b} \left[ \mathbf{Y}' + \left( z - \frac{4z^3}{3h^2} \right) \mathbf{R}'_y \right] + \frac{i\pi}{\lambda} \left[ \mathbf{X} + \left( z - \frac{4z^3}{3h^2} \right) \mathbf{R}'_x - \frac{16z^3}{3h^2 b} \mathbf{Z}' \right] \\ \left( 1 - \frac{4z^2}{h^2} \right) \mathbf{R}'_y + \frac{\pi i}{\lambda} \left( 1 - \frac{4z^2}{h^2} \right) \mathbf{Z} \\ \left( 1 - \frac{4z^2}{h^2} \right) \mathbf{R}'_x + \frac{2}{b} \left( 1 - \frac{4z^2}{h^2} \right) \mathbf{Z}' \end{bmatrix} \quad (10)$$

### c) Stiffness equations

It is assumed that the laminate is manufactured from an orthotropic layer of preimpregnated unidirectional fibrous composite materials. Neglecting  $\sigma_z$  for each layer, the stress-strain relations in the  $(x, y, z)$  coordinate system may be written as

$$\boldsymbol{\sigma} = \mathbf{Q} \boldsymbol{\varepsilon}_L \quad (11)$$

The components of  $\mathbf{Q}$  for each  $k$ -th laminate is discussed in Hinton and Owen [2]. The internal virtual work  $\delta W_i$  in a wavelength  $2\lambda$  of the strip due to the virtual displacement  $\delta \mathbf{d}$  may be expressed as

$$\delta W_i = \frac{\lambda b}{2\pi} \int_0^{2\pi} \int_{-1}^1 \int_{-\frac{h}{2}}^{\frac{h}{2}} \delta \boldsymbol{\varepsilon}_L^T \mathbf{Q} \boldsymbol{\varepsilon}_L d\xi d\eta dz \quad (12)$$

Substituting Eq. (9) into Eq. (12), the internal virtual work may be written in terms of displacements  $d$  as

$$\delta W_i = \frac{\lambda b}{2\pi} \int_0^{2\pi} \int_{-1}^1 \int_{-\frac{h}{2}}^{\frac{h}{2}} \text{Re}(\delta \mathbf{d}^T \mathbf{J} \boldsymbol{\Gamma}^T e^{i\eta}) \mathbf{Q} \text{Re}(\boldsymbol{\Gamma} \mathbf{J} d e^{i\eta}) d\xi d\eta dz \quad (13)$$

Performing the integration with respect to  $\eta$ , and after some mathematical manipulation involving complex arithmetic, Eq. (13) becomes

$$\delta W_i = \lambda \text{Re}(\delta \bar{\mathbf{d}}^T \mathbf{A} d) \quad (14)$$

where the bar denotes the complex conjugate and

$$\mathbf{A} = \frac{b}{2} \bar{\mathbf{J}} \left( \int_{-1}^1 \int_{-\frac{h}{2}}^{\frac{h}{2}} \bar{\boldsymbol{\Gamma}} \mathbf{Q} \boldsymbol{\Gamma} d\xi dz \right) \mathbf{J} \quad (15)$$

During the virtual displacements, the basic membrane forces acting on the four edges of a rectangle of width  $b$  and length  $2\lambda$  also work  $\delta W_m$ , and this is given by

$$\delta W_m = \delta \iiint \langle \sigma_T; \sigma_y; \tau \rangle \boldsymbol{\epsilon}_{NL} dx dy dz \quad (16)$$

On using the Eqs. (3, 4, 5, 7 & 8), and after some mathematical manipulation involving complex arithmetic, Eq. (16) becomes

$$\delta W_m = \lambda Re \left( \delta \bar{\mathbf{d}}^T \left( \sum_{r=1}^6 (\mathbf{B}_r + i\mathbf{C}_r) \right) \mathbf{d} \right) \quad (17)$$

Details of the terms  $\mathbf{B}_r$  and  $\mathbf{C}_r$  are given in Kassaei [22].

Once the strip stiffness  $\mathbf{A}$  and stability matrices  $\sum_{r=1}^6 (\mathbf{B}_r + i\mathbf{C}_r)$  have been derived for each thick strip, they can be assembled into the global matrices by using equilibrium and compability along nodal lines. Finally, the solution for the critical stress is obtained by allowing the determinant, obtained by subtracting the global stiffness and stability matrices, to vanish.

### 3. NUMERICAL RESULTS

#### a) General

The semi-analytical complex finite strip method for thick plates, employing the higher order shear deformation theory described in the previous section, was programmed on a desktop workstation. In order to ascertain the validity and accuracy of the method, square simply supported laminated plates with length-to-thickness ratio equal to 5 have been analysed. The thickness  $h$  is composed of equal thickness layers oriented at  $(0^\circ/90^\circ/0^\circ)$  and  $(45^\circ/-45^\circ/45^\circ/-45^\circ)$ , the material properties of each layer are  $(E_1=40.0E_2; G_{12}=G_{31}=0.6 E_2; G_{23}=0.5E_2; \mathcal{A}_{12}=0.25)$  and  $(E_1=40.0E_2; G_{12}=G_{23}=G_{31}=0.5E_2; \mathcal{A}_{12}=0.25)$ , respectively. The resulting dimensionless critical stresses are exhibited in Table 1 in comparison with the classical plate theory (CPT) based on the higher order shear deformation theory (HSDT) and the first order shear deformation theory (FSDT), and ordinary finite strip method (FSM) by Akhras *et al.* [13]. It can be seen that the complex finite strip method yields an acceptable accuracy as compared to the other solutions. It should be noted that only one harmonic was used in the analysis (Akhras *et al.* [13]).

Table 1. Non-dimensional critical stresses  $(\sigma_y)_{cr} a^2 / E_2 h^2$  of square cross-ply laminates

Method	$(0^\circ/90^\circ/0^\circ)$	$(45^\circ/-45^\circ/45^\circ/-45^\circ)$
HSDT	11.008	-
FSDT	10.525	15.117
Akhras <i>et al.</i> [1995]	10.674	14.895
Present	10.673	14.912

#### b) Long thick plate under compression

The local buckling of isotropic and laminated thick plates with longitudinal edges simply supported (SS) and clamped (CC) was studied using the complex finite strip method. The width-to-thickness ratio  $b/h$  is equal to 5. Table 2 shows the local buckling coefficient of both isotropic and laminated thick plate whose thickness layers are oriented at  $(45^\circ/-45^\circ)$ . The wavelength at which the calculations were performed are those corresponding to minimum buckling stress and are shown in parentheses. These results indicate the accuracy which can be achieved by subdividing the plate into a relatively small number of strips.

#### c) Long thick plate under shear

The advantage of the present method over the formulation of Akhras *et al.* [13] is the ease with which it can handle shear. The local buckling coefficients of thick isotropic and orthotropic plates with longitudinal

edges (SS) and (CC) subjected to pure shear stresses are shown in Table 3. The wavelengths at which minimum local buckling coefficients are obtained are shown in parentheses. Again, it is possible to obtain results with acceptable accuracy by subdividing the plates into a few strips.

Table 2. Local buckling coefficients of long isotropic and laminated thick plates under compression with width-to-thickness ratio ( $b/h=5$ .)

No. Strips	Thick isotropic plate		Laminated plate (45°/-45°)	
	SS ( $\lambda/b = 0.88$ )	CC ( $\lambda/b = 0.60$ )	SS ( $\lambda/b = 0.52$ )	CC ( $\lambda/b = 0.47$ )
1	3.2534	9.0750	9.9547	64.4271
2	3.1295	4.3970	9.8856	10.9431
3	3.1238	4.2339	9.8806	10.5668
4	3.1230	4.1846	9.8791	10.4363
6	3.1227	4.1443	9.8783	10.3326
8	3.1226	4.1270	9.8782	10.2931
10	3.1226	4.1178	9.8781	10.2749

Table 3. Local buckling coefficients of long isotropic and laminated thick plates under pure shear with width-to-thickness ratio ( $b/h=5$ .)

No. Strips	Thick isotropic plate		Laminated plate (45°/-45°)	
	SS ( $\lambda/b = 1.09$ )	CC ( $\lambda/b = 0.74$ )	SS ( $\lambda/b = 1.01$ )	CC ( $\lambda/b = 0.74$ )
1	5.0081	10.6156	13.7595	31.9860
2	3.8335	6.0354	10.9412	14.5636
3	3.6886	4.8779	10.6539	12.0956
4	3.6574	4.7184	10.5843	11.7452
6	3.6449	4.6369	10.5528	11.5754
8	3.6428	4.6111	10.5461	11.5304
10	3.6422	4.5989	10.5439	11.5127

#### d) Boundary conditions effects

By using the additional functions in the longitudinal direction [21], the procedure is deployed to investigate the effect of different boundary conditions on the local buckling of thick orthotropic plates whose loaded edges are either simply supported (SS), one end clamped and the other simply supported (CS), or one end clamped and the other guided (CG). The Variation of the local buckling coefficients  $k_a$ , obtained from the equation

$$k_a = \frac{\sigma_{cr}}{E_2} \left( \frac{b}{h} \right)^2 \quad (18)$$

against aspect ratio  $L/b$  for thick laminated plates whose longitudinal edges are SS, CC and CS are shown in Figs. 3, 4 and 5, respectively. It can be seen that the boundary conditions along the loaded edges substantially affect the value of  $k_a$  when  $L/b$  is less than 0.8, while the restraint of the loaded edges has little effect on the local buckling coefficient of long thick plates.

Figures 6 to 8 illustrate the variation of the shear local buckling  $k_s$  with aspect ratio for thick plates under pure shear whose longitudinal edges are SS, CC and CS, respectively. Three boundary conditions along the loaded edges have been considered, namely SS, CS and CG. Again, the local buckling coefficient is insensitive to large values of the aspect ratio. In all Figs. 3-8 the thickness  $h$  is composed of equal thickness layers oriented at ( $0^\circ/90^\circ/0^\circ$ ) and the length-to-thickness ratio is equal to 5.

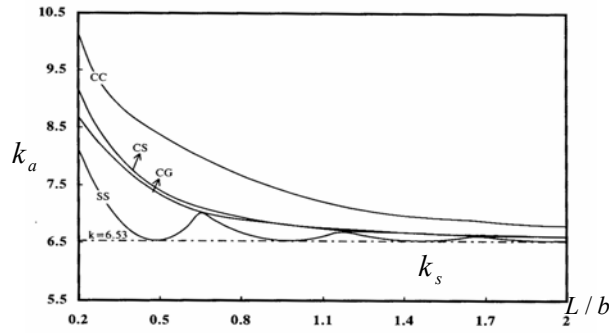


Fig. 3. Buckling coefficient for simply supported (SS) orthotropic plate in compression with layers oriented at  $(0^\circ/90^\circ/0^\circ)$  and  $b/h=5$

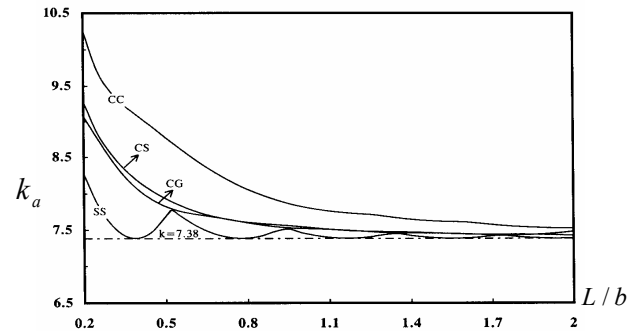


Fig. 4. Buckling coefficient for clamped (CC) orthotropic plate in compression with layers oriented at  $(0^\circ/90^\circ/0^\circ)$  and  $b/h=5$

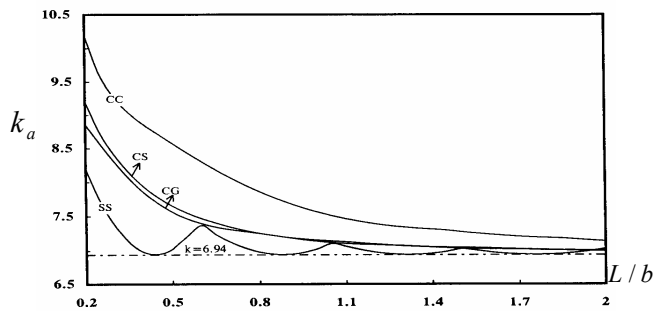


Fig. 5. Buckling coefficient for simply supported-clamped (SC) orthotropic plate in compression with layers oriented at  $(0^\circ/90^\circ/0^\circ)$  and  $b/h=5$

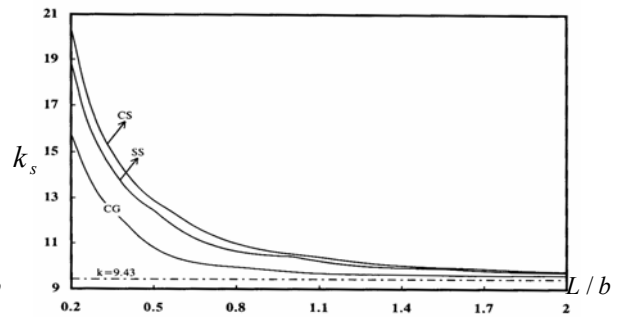


Fig. 6. Buckling coefficient for simply supported (SS) orthotropic plate in pure shear with layers oriented at  $(0^\circ/90^\circ/0^\circ)$  and  $b/h=5$

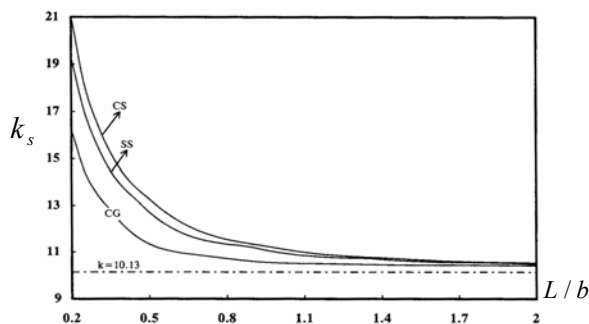


Fig. 7. Buckling coefficient for clamped (CC) orthotropic plate in pure shear with layers oriented at  $(0^\circ/90^\circ/0^\circ)$  and  $b/h=5$

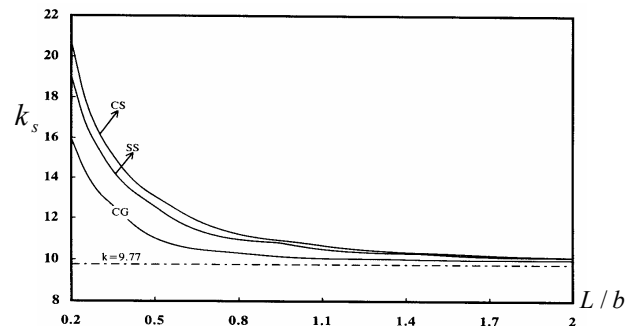


Fig. 8. Buckling coefficient for simply supported-clamped (SC) orthotropic plate in pure shear with layers oriented at  $(0^\circ/90^\circ/0^\circ)$  and  $b/h=5$

### e) Local buckling half-wave length

The variation of local buckling coefficient  $k_a$  against dimensionless buckling half-wavelength  $\lambda/b$  for a long orthotropic plate under uniform compression with the different length-to-thickness ratio is shown in Fig. 9, when thickness layers are oriented at  $(45^\circ/45^\circ/45^\circ/45^\circ)$ , and in Fig. 10 for the case when thickness layers are oriented at  $(45^\circ/45^\circ/45^\circ/45^\circ)$ . A plot of the local buckling coefficient  $k_s$  for a long orthotropic plate under uniform shear with the different length-to-thickness ratio when thickness layers are oriented at  $(45^\circ/45^\circ/45^\circ/45^\circ)$  is also shown in Fig. 11.

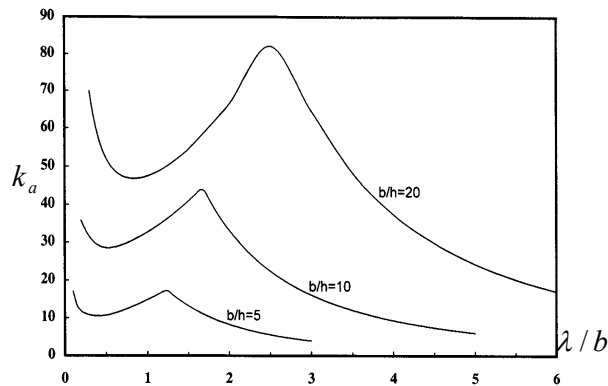


Fig. 9. Buckling coefficient Vs half-wavelength for simply supported orthotropic plate in compression with layers oriented at  $(45^\circ/-45^\circ/45^\circ/-45^\circ)$  and  $b/h=5$

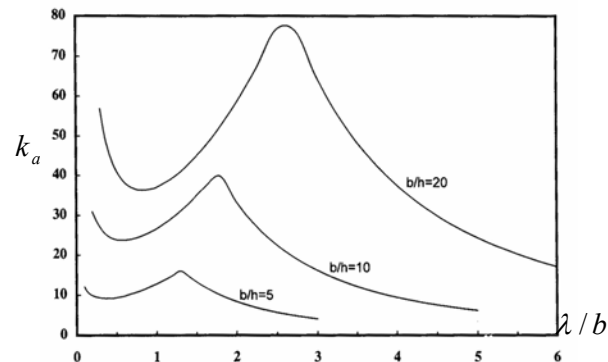


Fig. 10. Buckling coefficient Vs half-wavelength for simply supported orthotropic plate in compression with layers oriented at  $(45^\circ/-45^\circ/45^\circ/45^\circ)$  and  $b/h=5$

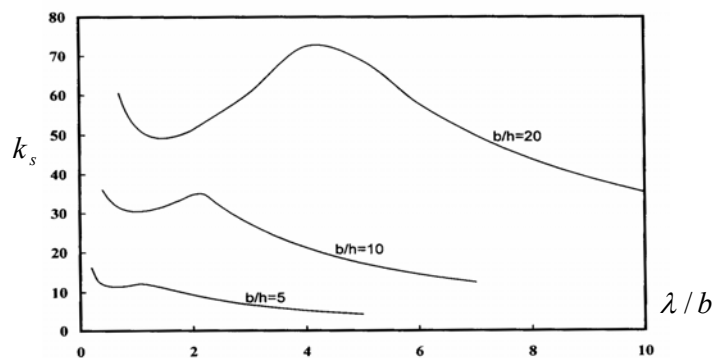


Fig. 11. Buckling coefficient Vs half-wavelength for simply supported orthotropic plate in pure shear with layers oriented at  $(45^\circ/-45^\circ/45^\circ/-45^\circ)$  and  $b/h=5$

It can be seen that the curves are sensitive to the length-to-thickness ratio  $b/h$ . For all cases, the curves exhibit the same characteristics, namely two limbs, the first has a minimum value of  $\lambda/b$  between 0.4 and 0.8. As the wavelength increases, the curves rise to a peak and beyond the peak, the local buckling coefficient decreases with increasing half-wavelength. As the curves show, the half-wavelength in which the minimum of the local buckling coefficients occurred increased to  $\lambda/b$ .

#### f) Local buckling interaction

The interaction curve for local buckling of thick orthotropic plate whose length-to-thickness ratio is 5 when thickness layers are oriented at  $(45^\circ/-30^\circ)$  under combined shear and longitudinal compression has been investigated. Figure 12 shows the buckling stresses  $\sigma_{Lcr}$  and  $\tau_{cr}$  normalized with respect to the values  $\sigma_{cro}$  and  $\tau_{cro}$  in pure compression and shear only respectively. This interaction curve was obtained by fixing the ratio between the compression and shear stress, and factoring this monotonically by a load factor in the analysis. Critical values of the local buckling load factor were computed over a range of half-wavelength and the minimum value at the local nadir was obtained.

The interaction curve for local buckling under combined shear and bending for a plate whose length-to-thickness ratio is 10 is given in Fig. 13. This curve was obtained by the method described above. It can be seen for Figs. 12 and 13 that the interaction between shear and compression is close to parabolic, while the interaction between shear and bending is close to circle, as is assumed in design for thin plates [23] and [24].

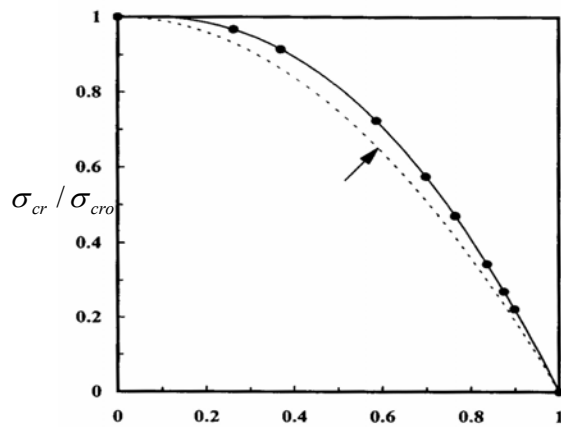


Fig. 12. Interaction curve for local buckling in shear and compression for simply supported orthotropic plate with layers oriented at  $(45^\circ/-30^\circ)$  and  $b/h=5$

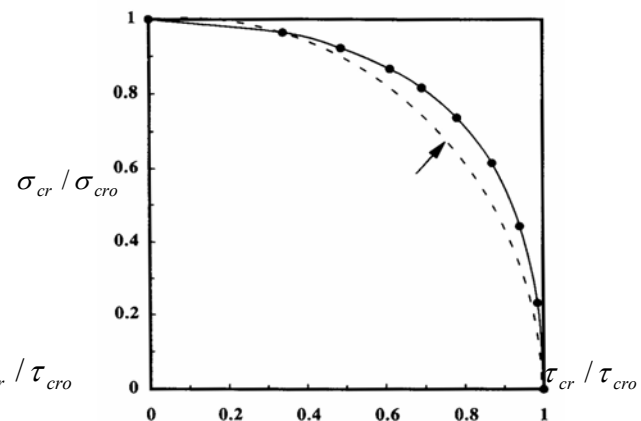


Fig. 13. Interaction curve for local buckling in shear and bending for simply supported isotropic plate with  $b/h=10$

#### 4. CONCLUSIONS

It has been shown that the complex finite strip method could be extended successfully to the analysis of thick plates. The method uses complex harmonic functions in the longitudinal direction, Hermitian cubic polynomials in the transverse direction and a parabolic distribution of the transverse shear strains through the thickness of the plate based on the higher-order shear deformation theory. As a result, slopes are continuous across the nodal lines between the finite strips. This method can predict accurate local buckling stress of very thick plates. The advantage of the method is the ease with which it can handle shear. Critical values of wavelength as a fraction of the plate width have been computed. Agreement with results quoted in the literature has been found for square laminates. The method has been used to calculate local buckling coefficients of thick composite long plates under compression and shear. Simply supported, clamped, simply supported-clamped thick orthotropic plates under compression and shear with different boundary conditions along the loaded ends have been studied. It was shown that although the restraint of the loaded edges in short thick plates has a considerable effect on the critical stresses, it has little effect on the buckling stress of long thick plates. The local buckling interaction between compression and shear was shown to be close to parabolic, and between pure bending and shear was shown to be close to circle.

#### NOMENCLATURE

$A$	strip stiffness matrix	$R_x, R_y$	interpolation matrices
$b$	plate width	$u, v$	membrane displacements
$B_r$ and $C_r$	strip stability matrices	$w$	flexural displacement
$d$	vector of perturbation displacement	$x, y, z$	Cartesian axes in Fig.1
$h$	plate thickness	$X, Y, Z$	interpolation matrices
$i$	$\sqrt{-1}$	$\Gamma$	strain matrix
$k_a$	local buckling coefficient in compression	$\epsilon_L$ and $\epsilon_{NL}$	linear and nonlinear strain
$k_s$	local buckling coefficient in shear	$\lambda$	local buckling half-wavelength
$L$	plate length	$\zeta$ and $\eta$	non-dimensional coordinates
$p$	vector of perturbation forces	$\sigma_{cr}$	critical stress for compression
$Q$	laminare property	$\tau_{cr}$	critical stress for shear
		$\psi_x, \psi_y$	rotations normal to the mid-plane

## REFERENCES

1. Zuriek, A. (1998). FRP Pultruded structural shapes. *Progress in Structural Engineering & Material*, 1(2), 143-149.
2. Hinton, E. & Owen, D.R. (1984). *Finite element software for plates and shells*. Pineridge Press, Swansea.
3. Chang, C. N. & Chang, F. K. (1988). Vibration analysis of thick plate with an interior cut-out by a finite element method. *J. Sound Vibr.*, 125(3), 477-486.
4. Noor, A.K. (1975). Stability of multilayered composite plates. *Fiber Science and Tech.* 8, 81-89.
5. Stein, M. (1985). Postbuckling of long plates under combined loading. *AIAA, J.*, 23, 1267-1272.
6. Nemeth, M. (1986). Importance of anisotropy on buckling of compression loaded symmetric composite plates. *AIAA, J.*, 24, 1831-1835.
7. Kant, T. & Kommineni, J. R. (1994). Geometrically non-linear transient analysis of laminated composite and sandwich shell with a refined theory and Co finite elements. *Comput. Struct.*, 52(6), 1243-1259.
8. Reddy, J. N. & Chandrashekhara, K. (1985). Geometrically non-linear transient analysis of laminated, doubly curved shells. *Int. J. Non-linear Mech.* 20, 79-90.
9. Reddy, J. N. & Chandrashekhara, K. (1985). Non-linear finite element models of laminated plates and shells. *In Finite Element in Computational Mechanics* (Edited by T. Kant), Pergamon Press, London, 189-209.
10. Sing, G., Venkateswara Rao, G. & Iyengar, N. G. R. (1994). Geometrically non-linear flexural response characteristics of shear deformable unsymmetrically laminated plates. *Comput. Struct.*, 53(1), 69-81.
11. Cheung, Y. K. (1976). *Finite strip method in structural analysis*. Pergamon Press, Oxford.
12. Zeggane, M. & Siridharan, S. (1991). Buckling under combined shear deformable laminated anisotropic plates using infinite strips. *Int. J. Numer. Meth. Engng.* 31, 1319-1331.
13. Akhras, G. Cheung, M. S. & Li, W. (1995). Vibration and stability analyses of thick anisotropic composite plates by finite strip method. *Struct. Engng. Mech.* 3(1), 49-60.
14. Daw, D. J. & Wang, S. (1994). Buckling of composite plates and plate structures using the spline finite strip method. *Composite Engng.*, 4, 1009-1117.
15. Daw, D. J. & Wang, S. (1995). Spline finite strip analysis of the buckling and vibration of rectangular composite laminated plates. *Int. J. Numer. Meth. Engng.* 37, 645-667.
16. Wang, S., & Daw, D. J. (1997). Spline finite strip analysis of the buckling and vibration of composite prismatic plate structures. *Int. J. Meth. Scie.*, 39, 1161-1180.
17. Azhari, M., Abdollahian, M. & Bradford, M. A. (2000). Local buckling of composite laminated plate assemblies using the spline finite strip method. *Advan. Struct. Engng.*, 3(2), 173-178.
18. Saadatpour, M. M., Azhari, M. & Bradford, M. A. (2002). Analysis of general quadrilateral orthotropic thick plates with arbitrary conditions by the Rayleigh-Ritz method. *Int. J. Numer. Meth. Engng.* 54, 1087-1102.
19. Plank, R. J. & Wittrick, W. H. (1974). Buckling under combined loading of thin-flat-walled structures by a complex finite strip method. *Int. J. Numer. Meth. Engng.* 8, 323-339.
20. Azhari, M. & Bradford, M. A. (1994). Local buckling by the complex finite strip method using bubble functions. *J. Eng. Mech. ASCE*, 120(1), 43-57.
21. Bradford, M. A. & Azhari, M. (1995). Buckling of plates with different end conditions using the finite strip method. *Comput. Struct.*, 56(1), 75-83.
22. Kassaei, K. H. (1998). Stability of thick composite laminated plates using the complex finite strip method. M.Sc Thesis, Dept. of Civil Engineering, Isfahan University of Technology, Isfahan, Iran.
23. Trahiar, N. S. & Bradford, M. A. (1991). *The behavior and design of steel structure*. 2<sup>nd</sup> edition, Chapman and Hall, London.
24. Bradford, M. A. & Azhari, M. (1994). Buckling modes in I-beams by a complex finite strip method. *Australian Civil Engrg. Trans.*, CE36(3), 219-225.